Paper No. 70. (quote when citing this article)
Eleventh World Conference on Earthquake Engineering
ISBN: 0 08 042822 3

FINITE-ELEMENT MODELLING OF UNBOUNDED MEDIA

JOHN P. WOLF and CHONGMIN SONG

Institute of Hydraulics and Energy, Department of Civil Engineering, Swiss Federal Institute of Technology Lausanne, CH-1015 Lausanne, Switzerland

ABSTRACT

Novel methods based on finite elements to model the unbounded medium in a dynamic medium-structure–interaction analysis are summarised. Applications in soil-structure interaction demonstrate the high accuracy and efficiency.

KEYWORDS

Far field; Finite element; Radiation condition; Soil-structure interaction; Transmitting boundary

INTRODUCTION

In a seismic soil-structure–interaction analysis the structure of finite dimensions interacts dynamically through the *structure-soil interface* with the soil of infinite dimensions, called the *unbounded medium* in the following. A typical example of such a dynamic unbounded medium-structure–interaction analysis is shown in Fig. 1. The structure which can include an adjacent irregular part of the medium can exhibit nonlinear behaviour. The unbounded medium must remain *linear*. In contrast to the bounded

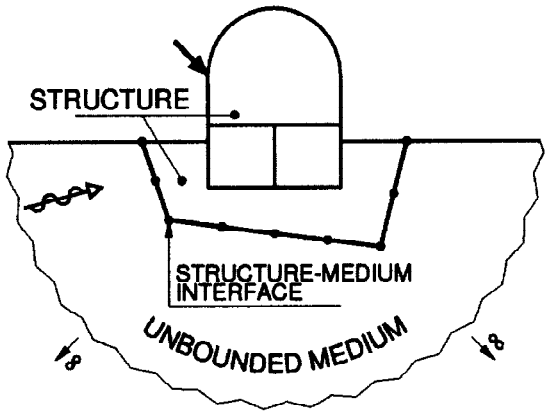

Fig. 1. Problem definition of dynamic unbounded medium-structure–interaction analysis

structure, the unbounded medium cannot be modelled with finite elements without a special treatment. Two procedures to model the unbounded medium exist. In the first, the *substructure method*, the

dynamic properties of the unbounded medium are represented rigorously by the interaction force-motion relationship defined on the structure-medium interface, which is global in space and time

$$\{R(t)\} = \int_0^t [M^\infty(t-\tau)]\{\ddot{u}(\tau)\}\mathrm{d}\tau \tag{1}$$

$[M^\infty(t)]$ is the *unit-impulse response matrix* of the unbounded medium relating the accelerations $\{\ddot{u}(\tau)\}$ to the interaction forces $\{R(t)\}$. In the second, the *direct method*, the medium adjacent to the structure-medium interface is modelled with finite elements up to the artificial boundary, which acts as a *transmitting boundary*, where an approximate boundary condition is introduced, which is local in space and time.

Recently, novel concepts based on the finite-element method to model the unbounded medium for the hyperbolic, parabolic and elliptic partial differential equations have been developed. They are described in detail with emphasis on wave propagation in the time and frequency domains in the book by Wolf and Song (1996). Applications to soil-structure–interaction analysis are summarised in this paper.

SIMILARITY-BASED FORMULATION

The boundary-element method is widely regarded as the most powerful procedure to model the unbounded medium in the substructure method of analysis. It requires a strong analytical and numerical background which the engineer who is familiar with finite elements has to acquire. As an alternative the *similarity-based formulation* using the finite-element method and standard matrix operations can be applied to calculated $[M^\infty(t)]$ in (1) (Part I of Wolf and Song, 1996). To explain the concept, a 2-dimensional half-plane with a discretized structure-medium interface is addressed (Fig. 2a). A similar

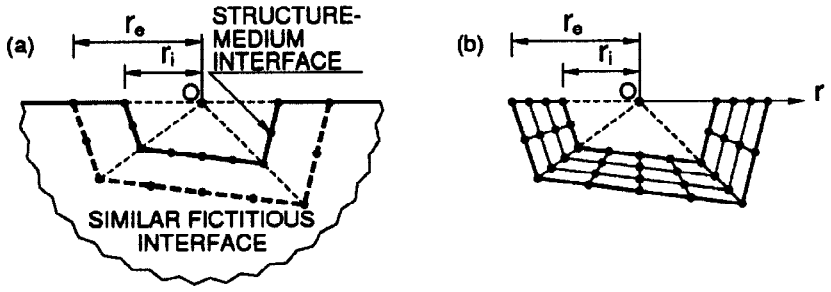

Fig. 2. Concept of similarity-based formulation

fictitious interface is constructed selecting the similarity centre O. The two similar interfaces are defined by their characteristic lengths r_i and r_e. A relationship between the unit-impulse response matrices at the two interfaces of the unbounded medium is derived using dimensional analysis. The region between the two interfaces is discretized with finite elements (Fig. 2b). Standard finite-element assemblage yields another relationship between the two unit-impulse response matrices. These two relationships permit $[M^\infty(t)]$ to be calculated.

Two implementations of the similarity-based formulation exist. The first, the *forecasting method* (Song and Wolf, 1995), makes use of the time delay of the waves propagating from one location to another separated by a few rows of finite elements (Fig. 2b), similar to weather and flood forecasting. Only the standard banded symmetric system of equations of the finite-element mesh is solved for each time step. No approximation in modelling the unbounded medium other than that of the finite-element method is introduced. Therefore, the forecasting algorithm *converges to the exact solution in the finite-element sense.* The second, the *consistent infinitesimal finite-element cell method* (Song and Wolf, 1996), works in the derivation with only one row of finite elements whose width measured in the radial direction is regarded as infinitesimal. After performing the limit of the width analytically, an equation for $[M^\infty(t)]$ is derived. In an actual calculation the discretization is limited to the structure-medium

interface (Fig. 3) leading to a *reduction of the spatial dimension by one.* The consistent infinitesimal

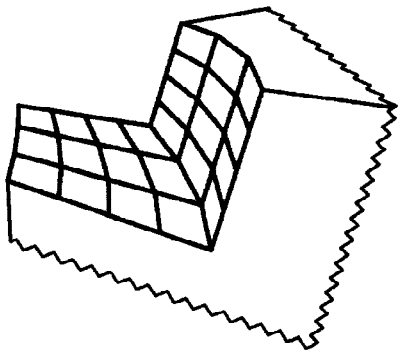

Fig. 3. Finite-element discretization of structure-medium interface in consistent infinitesimal finite-element cell method

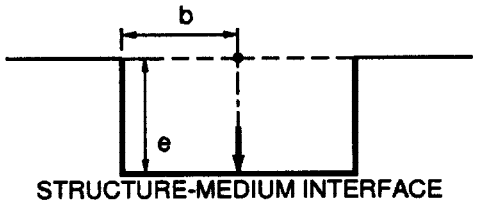

Fig. 4. Strip foundation with rectangular cross section embedded in transversely isotropic half-plane

finite-element cell method can be regarded as a *boundary-element method based on finite elements.* The procedure is *exact in the radial direction* and *converges to the exact solution in the finite-element sense in the circumferential directions.*

The similarity-based formulation captures the radiation condition at infinity using finite elements. For problems with a boundary extending from the structure-medium interface to infinity (such as a half-space with a free surface), this formulation automatically incorporates this boundary condition in contrast to the boundary-element method. Material inhomogeneities which satisfy similarity can also be processed without any additional effort. The similarity-based formulation can also calculate problems for which the fundamental solution (which is necessary in the boundary-element method) does not exist in closed form. This is, for example, the case for certain anisotropic materials. Only conventional static-stiffness and mass matrices of the finite elements are calculated, which does not involve singularities as in the boundary-element method.

The consistent infinitesimal finite-element method is used to analyse several examples with results available from other sources.

First, the vertical degree of freedom of a strip foundation with a rectangular cross section of width $2b$ and depth e ($e = b$) embedded in a transversely anisotropic half-plane is addressed (Fig. 4). The four ratios of the material constants are specified in Wolf and Song (1996). 24 3-node line elements of equal length are introduced in the discretization of the structure-medium interface. The unit-impulse response matrix $[M^{\infty}(t)]$ of order 98×98 is determined. To be able to compare with the results in the literature, a rigid interface is assumed. The vertical unit-impulse response coefficient $M^{\infty}(t)$ is calculated which is then transformed into the frequency domain. The resulting dynamic-stiffness coefficient non-dimensionalized by the shear modulus is decomposed into a spring coefficient $k(a_0)$ and damping coefficient $c(a_0)$ (Fig. 5). The agreement with the boundary-element solution of Wang and Rajapakse (1991) is good.

Second, as an example from actual practice, a railway tunnel intersecting a fault is addressed (Fig. 6a). The fault (Zone C) exhibits isotropic behaviour. The two zones of unbounded rock on both sides of the fault are modelled as transversely isotropic with a horizontal plane of isotropy. The material constants are specified in Wolf and Song (1996). A plane strain condition is assumed. The railway loads P results in concentrated forces as shown in Fig. 6a. The centre of similarity is selected on the middle line of the fault. As similarity is not satisfied exactly, small deviations of the locations of the interfaces between the fault and the rock occur (dashed lines in Fig. 6a). The surface is discretized with 31 isoparametric 3-node line elements (Fig. 6b). The unit-impulse response matrix $[M^{\infty}(t)]$ of order 124×124 is calculated. The displacements caused by a step function of the applied forces are determined step by step from (1). The deformed tunnel wall at a large time corresponding to statics (relative to the centre of the track) is

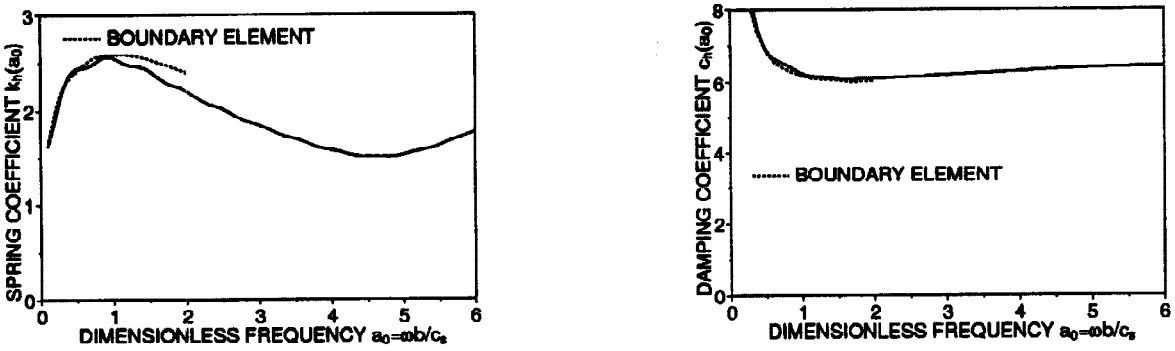

Fig. 5. Vertical dynamic-stiffness coefficient of rigid strip foundation embedded in half-plane

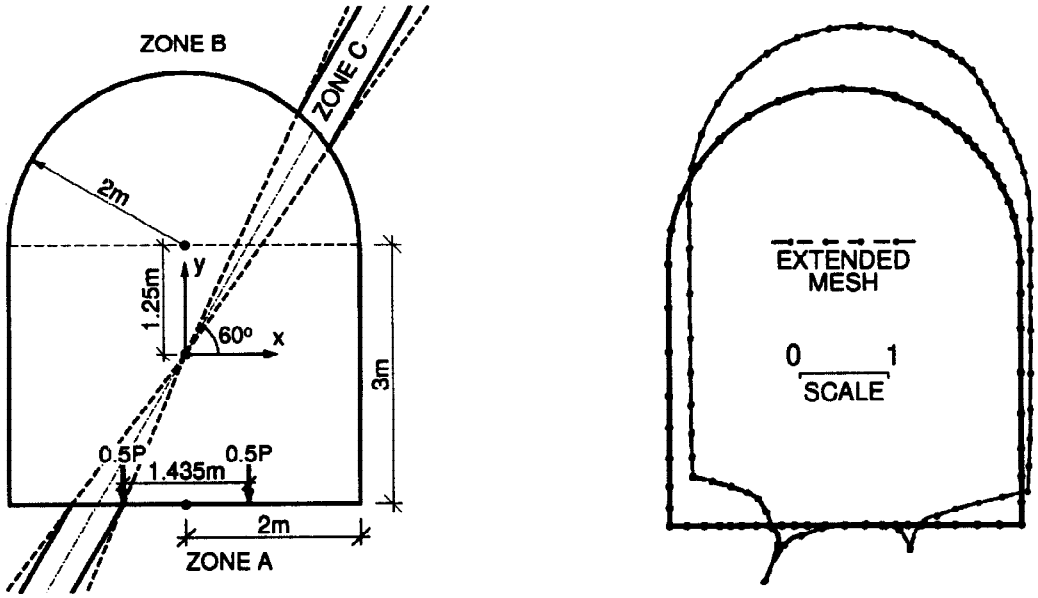

(a) geometry with similarity (b) deformed tunnel wall

Fig. 6. Tunnel in inhomogeneous transversely isotropic unbounded rock

plotted in Fig. 6b. The agreement with an extended-mesh solution is excellent. In passing, it is worth mentioning that the consistent infinitesimal finite-element cell method can also be applied directly for static problems (Wolf and Song, 1996).

Third, as a 3-dimensional problem a square prism of width $2b$ embedded with depth e ($e = 2/3b$) in a half-space with Poisson's ratio = 1/3 is addressed (Fig. 7a). The finite-element discretization of the structure-medium interface is shown in Fig. 7b. The vertical dynamic-stiffness coefficient is calculated from $[M^{\infty}(t)]$ as described in the first example. The non-dimensionalized spring and damping coefficients (Fig. 8) agree well with the boundary-element solution of Dominguez (1993). In addition, the transversely isotropic case with the material constants specified in Wolf and Song (1996) is addressed. The non-dimensionalized horizontal and vertical unit-impulse response coefficients plotted in Fig. 9 hardly deviate from the results of an extended-mesh analysis.

DAMPING-SOLVENT EXTRACTION METHOD

The dynamic-stiffness matrix $[S^{\infty}(\omega)]$ used in a frequency-domain analysis based on the substructure method can be calculated efficiently using the *damping-solvent extraction method* (Song and Wolf, 1994; Part II of Wolf and Song, 1996).

Its concept is best explained starting with a familiar process. To extract salt from the ground, water

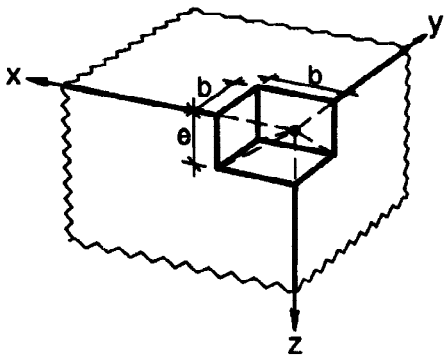

(a) geometry with similarity centre

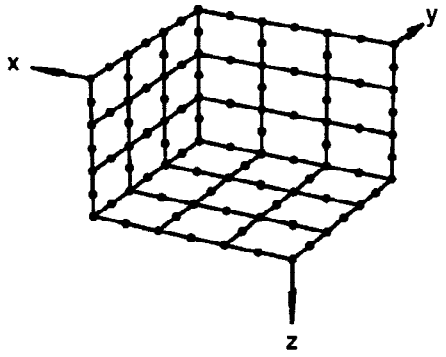

(b) finite-element discretization of structure-medium interface

Fig. 7. One quarter of square prism embedded in inhomogeneous half-space

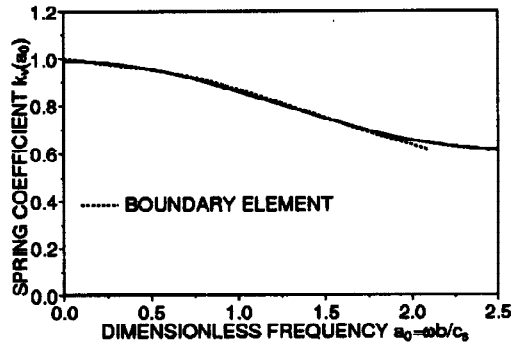

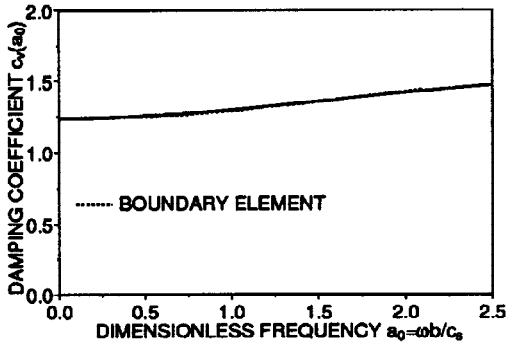

Fig. 8. Vertical dynamic-stiffness coefficient of rigid prism embedded in isotropic half-space

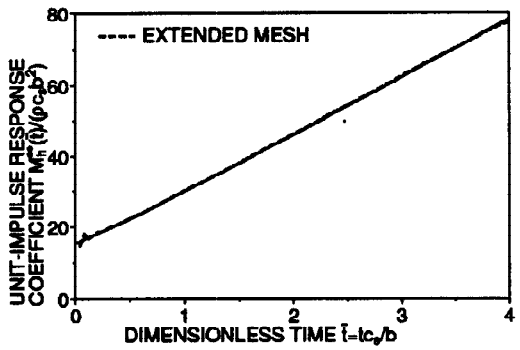

(a) horizontal

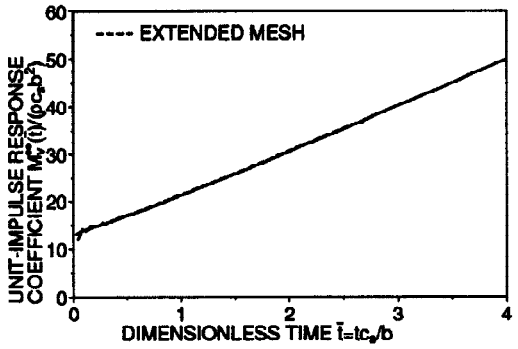

(b) vertical

Fig. 9. Acceleration unit-impulse response coefficient of rigid prism embedded in traversely isotropic half-space

is injected into the ground. The salt dissolves in the water which is then pumped to the surface. After evaporation of the water, the salt remains. To calculate the dynamic-stiffness matrix in the frequency domain of the undamped unbounded medium, damping is used as a solvent. Three steps are involved in the procedure.

In the *first step*, a *finite region of the unbounded medium* adjacent to the structure, a bounded medium, is modelled with *finite elements* (Fig. 10), whereby *damping* which is not present in the actual medium *is introduced artificially as a solvent.* Hysteretic material damping with the ratio ζ is used. The effect of this damping consists of reducing the amplitudes of the outgoing waves f propagating from the structure-medium interface towards the outer boundary and after reflection, diminishing the amplitudes of the reflected waves g, resulting in negligible amplitudes when reaching the structure-medium interface. The damping acting as a solvent thus leads to the structure-medium interface's motion depending only

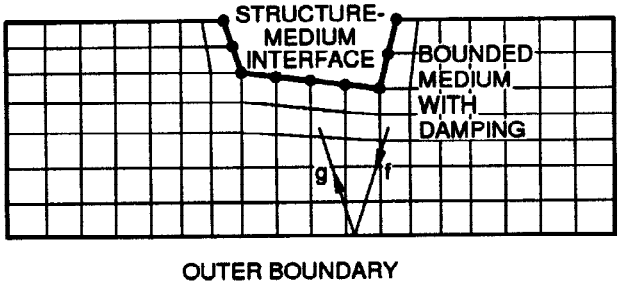

Fig. 10. Finite-element discretization of unbounded medium in first step of damping-solvent extraction method

on the outgoing waves f. The dynamic-stiffness matrix of the artificially damped bounded medium $[S_\zeta(\omega)]$ follows straightforwardly by eliminating all degrees of freedom which are not located on the structure-medium interface.

In the *second step*, the dynamic-stiffness matrix of the artificially damped bounded medium determined in the first step is assumed to be equal to the *dynamic-stiffness matrix of the unbounded medium with the same introduced artificial damping.* (The same is also assumed to apply for their first derivatives with respect to frequency).

In the *third step*, the influence of the *introduced artificial damping*, the solvent, on the dynamic-stiffness matrix *is extracted.* This elimination of the damping solvent can be performed for each element of the matrix independently from the others and for each frequency using a Taylor expansion

$$[S^\infty(\omega)] = \frac{1}{1+2\mathrm{i}\zeta}\left([S_\zeta(\omega)] + (\sqrt{1+2\mathrm{i}\zeta}-1)\omega\frac{\mathrm{d}[S_\zeta(\omega)]}{\mathrm{d}\omega}\right) \tag{2}$$

The computational effort is negligible.

The damping-solvent extraction method yields an accurate approximation of the dynamic-stiffness matrix of an unbounded medium by analysing the adjacent bounded medium only, which exhibits the same dynamic characteristics as the (bounded) structure.

As a stringent test of the damping-solvent extraction method, the out-of-plane (anti-plane) motion of a semi-infinite layer of constant depth d and shear-wave velocity c_s, which is a dispersive system with a cutoff frequency, is analysed (Fig. 11). To calculate the dynamic-stiffness matrix corresponding to a parabolic shape function with nodes 1 and 2, a finite region of length l ($l = 3d$) is discretized with finite elements and $\zeta = 0.2$ is selected. The dynamic-stiffness coefficient normalised and decomposed into $k(a_0)$ and $c(a_0)$ shown as a solid line in Fig. 12 agrees well with the exact solution specified in Wolf and Song (1996). For the sake of comparison, the undamped finite region of the same length with the

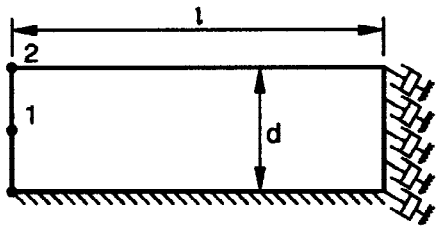

Fig. 11. Finite region of semi-infinite layer of constant depth

well-known viscous dashpots at the outer boundary is also evaluated (Fig. 11). This corresponds to the direct method of analysis based on the viscous dashpots serving as a transmitting boundary. As can be seen from the corresponding dynamic-stiffness coefficient shown as a dotted line, large deviations exist.

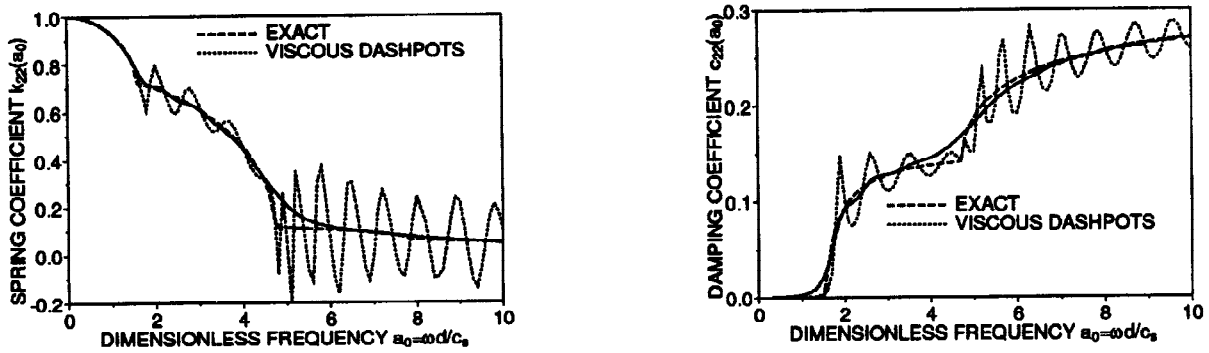

Fig. 12. Diagonal element of corner node of dynamic-stiffness matrix of semi-infinite layer

DOUBLY-ASYMPTOTIC MULTI-DIRECTIONAL TRANSMITTING BOUNDARY

The *doubly-asymptotic multi-directional transmitting boundary* (Wolf and Song, 1995; Part III of Wolf and Song, 1996) for use in a time-domain analysis based on the direct method is illustrated. To construct the doubly-asymptotic multi-directional transmitting boundary, the multi-directional outward plane-wave boundary condition is formulated for the interaction forces (and not for the displacements), whereby the contributions of the two limits covered rigorously by the doubly-asymptotic boundary are subtracted beforehand. The resulting boundary condition is discretized with finite differences leading to an explicit formulation, which is straightforwardly implemented in the finite-element method.

The doubly-asymptotic multi-directional transmitting boundary combines the advantages of the doubly-asymptotic and multi-directional formulations. It is *rigorous for the low-frequency limit* and the *high-frequency limit in the wave-propagation direction perpendicular to the artificial boundary and at all the preselected angles.* It is highly accurate for plane waves at intermediate frequencies and at other angles.

The semi-infinite rod on an elastic foundation (Fig. 13), another dispersive system with a cutoff frequency, is examined applying a rounded triangular displacement pulse $u_0(t)$ on the structure-medium interface for various transmitting boundaries. The details are specified in Wolf and Song (1996). 10 finite elements are used up to the artificial boundary. The interaction force $R(t)$ is calculated. The result of the doubly-asymptotic multi-directional transmitting boundary shown as a solid line in Fig. 14 is much closer to the extended mesh solution than those of the viscous dashpots and the multi-directional formulation used as transmitting boundaries.

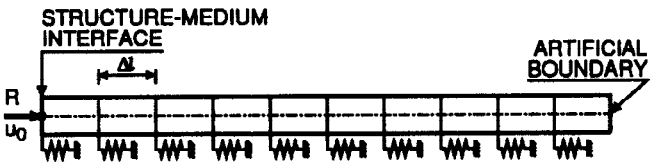

Fig. 13. Finite-element mesh up to artificial boundary of semi-infinite rod on elastic foundation

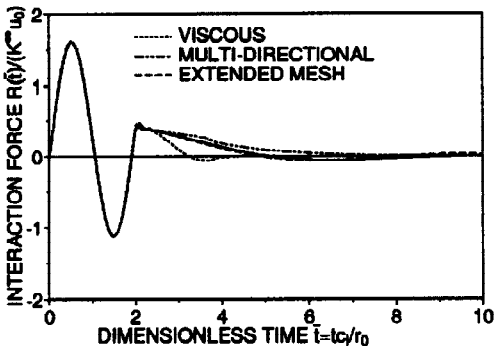

Fig. 14. Interaction force of semi-infinite rod on elastic foundation

As a two-dimensional example the in-plane motion of a semi-infinite wedge with an opening angle of $\alpha = 30°$ shwon in Fig. 15a is addressed.

A horizontal displacement $u_0(t)$ varying linearly and zero vertical displacement are prescribed. The finite-element mesh up to the artificial boundary is shown in Fig. 15b. The corresponding equivalent

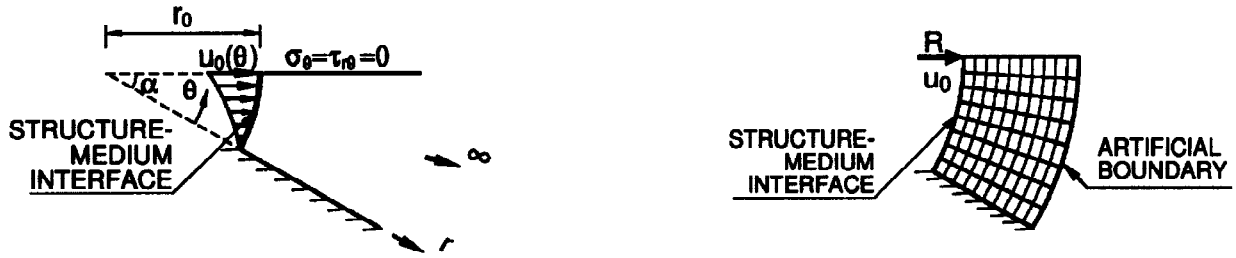

(a) problem definition (b) finite-element mesh up to artificial boundary

Fig. 15. Semi-infinite wedge with prescribed horizontal displacement

interaction force $R(t)$ is calculated. The result of the doubly-asymptotic multi-directional transmitting boundary hardly deviates from that of the extended mesh (Fig. 16a), in contrast to those of other transmitting boundaries (Fig. 16b).

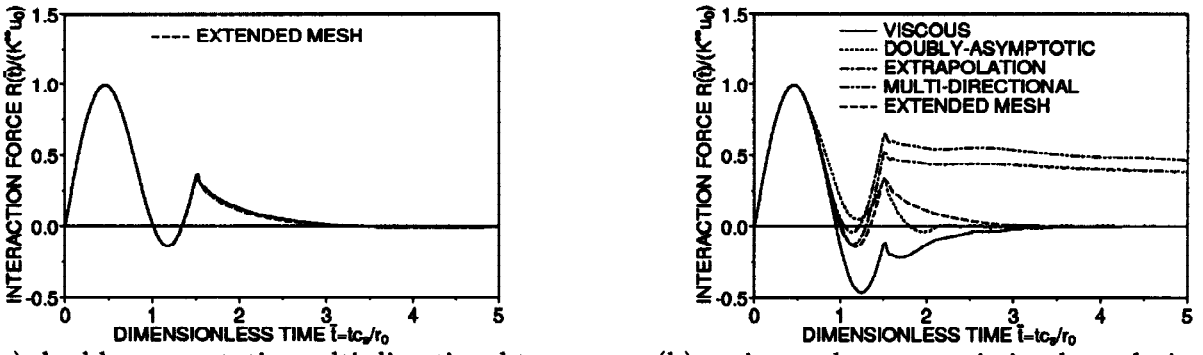

(a) doubly-asymptotic multi-directional transmitting boundary (b) various other transmitting boundaries

Fig. 16. Interaction force of semi-infinite wedge

REFERENCES

Dominguez, J. (1993) *Boundary Elements in Dynamics*, Computational Mechanics Publications, Southampton.

Song, Ch. and Wolf, J. P. (1994) Dynamic stiffness of unbounded medium based on damping-solvent extraction, *Earthquake Engineering and Structural Dynamics*, *23*, 169–181.

Song, Ch. and Wolf, J. P. (1995) Unit-impulse response matrix of unbounded medium by finite-element based forecasting, *International Journal for Numerical Methods in Engineering*, *38*, 1073–1086.

Song, Ch. and Wolf, J. P. (1996) Consistent infinitesimal finite-element cell method: three-dimensional vector wave equation, *International Journal for Numerical Methods in Engineering*, (in press).

Wang, Y. and Rajapakse, R. K. N. D. (1991) Dynamics of rigid strip foundations embedded in orthotropic elastic soils, *Earthquake Engineering and Structural Dynamics*, *20*, 927–947.

Wolf, J. P. and Song, Ch. (1995) Doubly asymptotic multi-directional transmitting boundary for dynamic unbounded medium-structure—interaction analysis, *Earthquake Engineering and Structural Dynamics*, *24*, 175–188.

Wolf, J.P. and Song, Ch. (1996). *Finite-Element Modelling of Unbounded Media*, John Wiley & Sons Ltd.